Phenanthroline impairs βAPP processing and expression, increases p53 protein levels and induces cell cycle arrest in human neuroblastoma cells

Subhamita Maitra, Wannapa Sornjai, Duncan Smith, Bruno Vincent

Phenanthroline impairs βAPP processing and expression, increases p53 protein levels and induces cell cycle arrest in human neuroblastoma cells

Subhamita Maitra[1], Wannapa Sornjai [1], Duncan R. Smith[1] and Bruno Vincent[1,2,*]

[1] Institute of Molecular Biosciences, Mahidol University, Nakhon Pathom, 73170 Thailand

[2] Centre National de la Recherche Scientifique, 2 rue Michel Ange, 75016 Paris, France

Running title: Effects of phenanthroline on βAPP and p53 biology

[*]Address correspondence to: Bruno Vincent (Tel: +66 (0)2441 9003-7 (ext 1451); Fax: +66 (0)2441 1013; email: bruno.vin@mahidol.ac.th)

Keywords: Alzheimer's disease; βAPP; secretase; p53; Calpain; Cell cycle arrest

Abbreviations: ADAM, A Disintegrin And Metalloprotease; HEK, Human Embryonic Kidney; AICD, APP IntraCellular Domain; *h*DM2, *human* Double Minute 2; DMEM, Dulbecco's Modified Eagle's Medium; ECL, Enhanced ChemiLuminescence; HRP, HorseRadish Peroxidase; SDS, Sodium Dodecyl Sulfate; BACE1, Beta-site APP Cleaving Enzyme 1; EDTA, EthyleneDiamineTetraacetic acid ; TCA, TriChloroacetic Acid; MTT, 3-(4,5-dimethylthiazol-2-yl)-2,5-diphenyltetrazolium bromide; PI, Propidium Iodide; MDM2, Mouse Double Minute 2; PDGF, Platelet-Derived Growth Factor

Abstract

Mis-functional βAPP processing is deemed to be the major phenomenon resulting in increased neuronal cell death, impaired neurogenesis and the loss of synapses, which eventually manifest as the complex symptoms of Alzheimer's disease. Despite of several milestones having been achieved in the field of drug development, the stigma of the disorder as an incurable disease still remains. Some ADAM proteases mediate the physiological non-amyloidogenic α-secretase processing of βAPP that generates neuroprotective sAPPα production. Earlier studies have also pointed out the role of p53 in Alzheimer's disease neuropathology, although a direct link with metalloprotease activities remains to be established. In this study, we explored the consequences of α-secretase inhibition on p53 status in cultured human neuroblastoma SH-SY5Y cells by means of specific inhibitors of ADAM10 and ADAM17 and the metal chelator and general metalloprotease inhibitor phenanthroline. We establish that, beyond the ability of all inhibitors to affect sAPPα production to varying degrees, phenanthroline specifically and dose-dependently lessened βAPP expression, a phenomenon that correlated with a strong increase in p53 protein levels and a concomitant decrease of the p53-degrading calpain protease. Furthermore, treatment of cells at concentrations of phenanthroline similar to those inducing increased levels of p53 induced cell cycle arrest leading to apoptosis. Altogether, our results identify new roles of phenanthroline in perturbing βAPP, p53 and calpain biology, and suggest that the use of this compound and its derivatives as antimicrobial and anti-cancer therapies might trigger Alzheimer's disease pathogenesis.

1. Introduction

Alzheimer's disease (AD) is one of the leading causes of an increased geriatric health burden across the globe. Being a multi-factorial complex disorder, it is characterized by the manifestation of several cellular dysfunctions such as oxidative stress, protein aggregation, mitochondrial defects and neuro-inflammation (Long and Holtzman, 2019). The prime triggering event is believed to be an increase in the amyloidogenic processing of the amyloid precursor protein (βAPP) leading to an excessive Aβ production, the formation of toxic soluble Aβ oligomers that gradually give rise to aggregated/fibrillar Aβ and ultimately to senile plaques (Benilova et al., 2012).

Although neuronal dysfunction and subsequent massive neuronal loss is the end point of the pathology leading to the cognitive decline of AD patients, it would be too simplistic to ascribe the AD pathology to a single causative factor. As an example, a tendency to cell cycle re-entry, immunological sensitization and apoptosis have also been shown to be modulators of disease initiation (Zhu et al., 2004). In the context of the cell cycle, p53, as the guardian of the genome, plays a crucial role in maintaining the check point and passage of cells into the next phase and altered p53 activity can lead to either arrested cell proliferation or unregulated hyperplasia (Vousden and Prives, 2009). Moreover, a clear involvement of p53 in cell cycle re-entry, a phenomenon that is thought to constitute a common pathway in apoptosis in neurodegeneration, has been shown (Folch et al., 2012).

For these reasons, the possible involvement of p53 in neurological diseases and more especially in AD pathogenesis has led to growing interest over the past 25 years (Jazvinscak Jembrek et al., 2018). Indeed, and despite a very complex biological profile including a dual implication in cell death and longevity, it has been shown that p53 protein levels are highly elevated in the temporal cortex (Kitamura et al., 1997; Alves da Costa et al., 2006) and in the superior temporal gyrus (Hooper et al., 2007) of AD patients. Moreover, while higher levels

of p53 were found in peripheral lymphocytes of AD patients when compared to controls (Tan et al., 2012), it was also observed that p53 is conformationally altered in mononuclear cells of AD individuals when compared to non-AD subjects (Lanni et al., 2008), thereby suggesting roles for p53, phospho-p53 and p53 mutants as new putative markers of the pathology. In this context, it was also reported that blood lymphocytes in AD patients showed less sensitivity to the G1/S checkpoint and an anomalous conformation of p53 (Zhu and Jia, 2010). Finally, the fact that p53 was found to phosphorylate tau in an indirect way further links p53 biology to AD pathogenesis (Hooper et al., 2007).

At the molecular level, the p53 promoter is trans-activated by intracellular $A\beta_{1-42}$ (Ohyagi et al., 2005), while p53 is associated with the functions of all members of the heterotetrameric γ-secretase complex (Checler et al., 2010) and is under the positive transcriptional control of the γ-secretase-dependent βAPP-derived metabolite AICD (Alves da Costa et al., 2006). In addition, it has been established that the overexpression of βAPP in human HEK293 cells could alter p53 conformation (Uberti et al., 2007). In return, it was established that p53 can down regulate βAPP transcription (Cuesta et al., 2009). These results taken as a whole tend to indicate that there exist several functional networks linking p53 to βAPP, to βAPP-derived metabolites and to the molecular machinery responsible for the γ-cleavage of βAPP.

It is also interesting to note that p53 is under the control of the metal chelator and redox sensitive 1,10-phenanthroline compound (also called orthophenanthroline; Phe). Firstly, Phe, when used at millimolar concentrations, reversibly induces wild-type p53 to adopt a mutant conformation, thereby suggesting that metal ions stabilize wild-type p53 folding to favor its tumor suppressor properties (Hainaut and Milner, 1993). Secondly, Phe, via its metal chelating properties, stimulates endogenous wild-type p53 transcriptional activity as evidenced by a dose-dependent promoter transactivation in two murine tumor cell lines (Sun et al., 1997). Finally, and more recently, it was demonstrated that a synthetic organometallic

compound encompassing Phe was able to disrupt p53/*h*DM2 interaction and consequently increased the amount of free p53 in human melanoma A375 cells (Liu et al., 2016). However, none of these studies were performed in cells of a neuronal origin, or with a neuronal phenotype, although a positive effect of potent iron chelators on p53 expression and DNA-binding activity was demonstrated in human neuroblastoma and neuroepithelioma cells (Liang and Richardson, 2003).

Because Phe, due to its zing chelating activity, is also supposed to inhibit the ADAM (A Disintegrin And Metalloprotease) family of proteases, several of which being responsible for the non-amyloidogenic α-secretase processing of βAPP (Vincent and Checler, 2012), the present study was aimed at investigating the effect of Phe as well as some specific α-secretase inhibitors on βAPP processing and expression, p53 levels and cell cycle arrest in a human neuroblastoma cell line.

We here show that Phe inhibits α-secretase catalytic activity, represses βAPP transcription, strongly augments p53 protein levels, most likely via a diminution of p53-degrading calpain2 expression, and dose-dependently triggers cell cycle arrest in SH-SY5Y cells. Overall, Phe, via its dual action on βAPP and p53 biology, leads to an exacerbation of deleterious events reminiscent of AD pathology, thereby providing a molecular mechanism suggesting why physiological impairment of metal homeostasis, and zinc in particular, might represent a risk to develop AD.

2. Materials and Methods

2.1. Reagents

Polyclonal anti-ADAM10 (AB19026) and anti-ADAM17 (AB19027) were from Millipore (Bedford, MA, USA). Monoclonal anti-BACE1 (ab108394) was from Abcam

(Cambridge, UK). Polyclonal anti-βAPP antibody (A8717), monoclonal anti-β-actin (A2228), GI254023X, dimethyl sulfoxide (DMSO), SDS and sodium bicarbonate were from Sigma (St Louis. MO. USA). Monoclonal anti-p53 (sc-126) was from Santa Cruz Biotechnology Inc. (Santa Cruz, CA, USA). Polyclonal anti-calpain2 (2539S) was from Cell Signaling (Beverly, MA. USA). Monoclonal anti-β-amyloid (2B3), which was used to specifically detect sAPPα was from IBL (Minneapolis, MN, USA). DMEM complete medium, penicillin-streptomycin (Pen/Strep) mix and foetal bovine serum were from Invitrogen (Carlsbad, CA, USA). Tris buffer and Glycine were from VWR Amresco lifesciences (Solon, CA, USA). Skim milk powder was from Biobasic (Singapore). ECL reagent and ammonium persulphate were from GE Health care (Pisataway, NJ, USA). Phenanthroline and TAPI-1 were from Calbiochem (San Diego, CA, USA).

2.2. Cell lines and treatments

SH-SY5Y cells were maintained in 100mm petri dishes (purchased from Corning incorporated) with DMEM (12800-017), containing $NaHCO_3$, 10% FBS and 1% Pen/Strep. For experiments dealing with sAPPα production and western blot analyses, cells were cultured in 35mm-dishes until cells reach 80% confluence and were pre-incubated without (control) or with the ADAM10 specific inhibitor GI254023X (10μM), the ADAM17 specific inhibitor TAPI-1 (10μM) or various concentrations of the metal chelator and general metalloproteinase inhibitor phenanthroline (Phe) for 30 minutes at 37^0C in 1ml of serum-free DMEM.

2.3. sAPPα secretion and detection

Following treatments, DMEM was removed and cells were incubated under the same conditions in fresh DMEM and allowed to secrete for 5 hours. After the completion of 5

hours, 10% TCA precipitation of the whole medium was performed and the precipitate was subjected to electrophoresis through 10% SDS-PAGE gels, transferred onto nitrocellulose membranes (120 min, 100 volts), incubated in 5% non-fat milk blocking solution for 30 min and incubated overnight at 4°C with the human-specific anti-sAPPα antibody 2B3 (1µg/ml). After three washes with PBST (PBS containing 0.05% Tween 20), membranes were then incubated with a HRP-conjugated anti-mouse IgG antibody, rinsed three times with PBST incubated with ECL reagent and signals were detected using an Azure c400 (Azure Biosystems, Dublin, CA, USA). Band densities were measured with the Image J software (http://imagej.nih.gov/ij/).

2.4. Western blot analyses

15-30 µg (ADAM10, BACE1, βAPP) or 30-40µg (p53 and calpain 2) protein were loaded onto 10% of SDS-PAGE gels which were run at 100 volts for 1-2.5 hours. Proteins were then transferred onto nitrocellulose membrane for 90-140 minutes at 90 volts. Protein transfer was verified by Ponceau red staining, and nitrocellulose membranes were subsequently incubated in 5% non-fat milk blocking solution for 45 minutes. Membranes were then incubated with primary antibodies directed against ADAM10 (dilution 1/500), ADAM17 (dilution 1:500), BACE1 (dilution 1/1000), βAPP (dilution 1/2000), p53 (dilution 1/500), calpain2 (dilution 1/500) or β-actin (dilution 1/5000) on a platform shaker overnight at 4°C. After 3 washes with PBST, membranes were incubated with a HRP-conjugated anti-rabbit (ADAM10, ADAM17, βAPP, BACE1 and calpain2) or anti-mouse (p53 and β-actin) secondary antibody (1/3000) for 2h, rinsed 3 times with PBST and processed as described above. All protein levels were normalized using β-actin as an internal standard.

2.5. α-secretase fluorimetric assay on intact cells

SH-SY5Y cells were cultured in 35mm-dishes coated with polylysine (10µg/ml) until cells reached 80% confluence. Cells were then incubated for 30 min at 37^0C in the absence (control) or in the presence of the indicated concentrations of Phe or with GI254023X (ADAM10-specific inhibitor, 10µM) in 1.5ml of PBS. Then, the α-secretase-specific JMV2770 substrate (10µM) (Alfa Cissé et al., 2006) was directly added into the media and cells were maintained at 37^0C. Every 15 minutes, 100µl of media were removed and the α-secretase-catalytic activity was recorded in black 96-well plates at 320nm and 420nm excitation and emission wavelengths respectively.

2.6. Real-time quantitative polymerase chain reaction (qPCR)

Following a 5.5 hours treatment, total RNA was extracted and purified with the PureLink RNA mini kit (Ambion, Life Technologies, Austin, TX, USA). Real-time PCR was performed with 100ng of total RNA using the QuantiFast SYBR Green RT-PCR kit (Qiagen, Singapore) detector system (ABI Quant Studio 5, Thermo Fisher Scientific, Waltham, MA, USA) and the SYBR Green detection protocol. The 2x QuantiFast SYBR Green RT-PCR master mix, QuantiFast RT mix, QuantiTectPrimer Assay and template RNA were mixed and the reaction volume was adjusted to 25µl using RNase-free water. The specific primers were designed and purchased from Qiagen. Each primer consists of a 10x QuantiTect Primer Assay containing a mix of forward and reverse primers for specific targets: Hs_βAPP_1_SG (QT00050554 human βAPP), Hs_p53_1_SG (QT00060235, human p53), Hs_Calpain2_1_SG (QT00048006, human calpain2) and Hs_GAPDH_1_SG (QT00079247, human GAPDH).

2.7. Cell viability assay

Cells were seeded in 96-well polystyrene-coated tissue culture plates (Corning) over night. Proper attachment and confluence of the cells were confirmed by checking under a microscope. Media was removed and cells were treated with inhibitors at various concentrations in quadruplicate for 5 hours with control cells being treated with vehicle (0.1% DMSO). Media was then removed and cells were washed with sterile milli-Q water. Then, (3-(4,5-dimethylthiazol-2-yl)-2,5-diphenyltetrazolium bromide (MTT) was added (0.5mg/ml) for 1.5 hours. Formazan crystals formation was then checked under a microscope and the media was replaced by 100% DMSO until the purple crystals dissolved. Absorbance was measured at 595nm.

2.8. Sub G1 and cell cycle analysis by flow cytometer

After 24 h of treatment, SH-SY5Y cells were trypsinized and dispersed into single cells. All treated cells were collected and washed with ice cold 1X PBS. Washed cells were fixed and immobilized in ice cold 70% ethanol until required. For staining, fixed cells were washed twice with ice cold 1X PBS and then subsequently incubated with a propidium iodide (PI) staining solution containing 100 µg/mL RNase A, 0.1% Triton-X 100 and 10 µg/mL PI for 30 min. Stained cells were analyzed using a FACS Calibur flow cytometer (BD Biosciences, Franklin Lakes, NJ) and CELLQuest Pro software (BD Biosciences).

2.9. Statistical analysis

Statistical analyses were performed with the Prism software (GraphPad, San Diego, USA) using an unpaired t-test for pair wise comparisons.

3. Results

3.1. Phe diminishes sAPPα production, α-secretase activity and βAPP immunoreactivity without modifying secretase levels

In a first set of experiments, we examined the effect of the redox-sensitive, metal chelator and general metalloprotease inhibitor phenanthroline (Phe) as well as the ADAM10-specific inhibitor GI254023X and the ADAM17-specific inhibitor TAPI-1 on the non-amyloidogenic α-secretase processing of βAPP in cultured human SH-SY5Y neuroblastoma cells. The concentrations of GI254023X and TAPI-1 were chosen based on those used in the literature to inhibit their respective target in an optimal manner (Jacobsen et al., 2010; Kim et al., 2008). The results showed that all three compounds impair sAPPα secretion although to different extents (Fig. 1A). Thus, while GI254023X reduces the sAPPα-forming activity by 75%, TAPI-1 only moderately (about 20%), although significantly, prevents sAPPα production (Fig. 1A). Regarding Phe, we observed a moderate but significant reduction of sAPPα release, most likely due to its zinc-chelating properties, which is comparable to the result obtained with TAPI-1 (Fig. 1A). More surprisingly, Phe, but neither GI254023X nor TAPI-1, was able to significantly lower βAPP immunoreactivity (Fig. 1A). Therefore, the observed rather low ability of Phe to reduce sAPPα secretion might be due, at least partly, to a concomitant Phe-dependent depletion of the βAPP substrate. Because of this dual inhibitory effect of Phe on sAPPα production and βAPP levels, we wanted to ascertain whether Phe genuinely impairs α-secretase catalytic activity under our experimental conditions. Indeed, incubation of cultured SH-SY5Y cells with 100µM Phe flattens the curve representing the time-dependent hydrolysis of the α-secretase-specific fluorimetric substrate JMV2770 (Fig. 1B) and overall displayed a significant (50%) loss of α-secretase activity when compared to untreated cells (Fig. 1B, insert), a higher ratio than that obtained when sAPPα production was monitored (27%) (Fig. 1A). Finally, close examination of the impact of the three inhibitors on

the immunoreactivities of the two α-secretases ADAM10 and ADAM17 as well as the β-secretase BACE1 showed that none of them were able to significantly modify protein levels (Fig. 1C).

3.2. Phe dose-dependently decreases βAPP at a transcriptional level without interfering with cell survival

Following our original observation that Phe lessens βAPP protein immunoreactivity, we then wanted to examine whether the compound exerts an effect in a dose-dependent manner. Beyond confirming the inefficiency of GI254023X and TAPI-1 in this paradigm, treatment of SH-SY5Y cultured cells with a broad range of Phe concentrations (1nM to 100μM) led to a gradual decrease of βAPP protein levels that proved to be statistically significant at 10 and 100μM when compared to untreated control cells (Fig. 2A). Although the western blot data showed a dose-dependent βAPP protein down-regulation, it did not indicate whether it acts at a transcriptional or post-transcriptional level. To answer this question, we performed quantitative real-time PCR and showed that Phe negatively controls βAPP mRNA levels, in agreement with what is observed at the protein level (Fig. 2B). This set of data led us to compare the effect of the ADAM10 specific inhibitor GI254023X and Phe depending on whether we consider the α-secretase catalytic activity per se or the non-amyloidogenic processing of βAPP. Indeed, while both compounds significantly inhibited JMV2770 hydrolysis, although to different degrees (Fig. 2C), only GI254023X showed the ability to modify the sAPPα/βAPP ratio (Fig. 2D), thereby revealing an atypical impact of Phe with regard to the biology of βAPP. In order to rule out possible interference of Phe with βAPP processing/expression due to non-specific toxicity, we measured the effect of Phe at the highest concentrations triggering βAPP down regulation using the MTT assay. There were no

changes in cell death following 5.5 hours treatment, whatever the conditions considered, when compared to control (Fig. 2E), meaning that neither GI254023X nor TAPI-1 or Phe are toxic per se under these conditions.

3.3. Phe strongly and dose-dependently increases p53 protein amounts at a post-transcriptional level

We then searched for a cellular effector that could operate as a link between Phe and βAPP and our attention focused on p53, which can down-regulate βAPP (Cuesta et al., 2009) and is under the positive control of Phe as previously reported (Liu et al., 2016). We first showed that p53 protein levels were significantly increased in cultured SH-SY5Y cells incubated for 5.5 hours with 100µM Phe but were unchanged upon GI254023X or TAPI-1 treatment (Fig. 3A). Further analysis showed that Phe triggers an augmentation of p53 at 10 and 100µM (Fig 3B), a profile matching the one obtained for the Phe-dependent decrease in βAPP protein and mRNA levels (Fig. 2A-B). In an attempt to determine whether Phe stimulates p53 at a transcriptional level, we conducted real-time PCR experiments and unexpectedly observed a significant decrease of p53 mRNA levels at the concentrations strongly increasing p53 immunoreactivity (Fig. 3C). Nevertheless, these results indicate that Phe induces an increase of p53 immunoreactivity through a post-transcriptional mechanism, most likely resulting from a gain of stability of the p53 protein.

3.4. Phe transcriptionally represses the expression of the p53-degrading calpain-2 protease

One possible factor that could connect Phe to p53 is calpain, a calcium-activated protease that is able to cleave p53 and therefore most likely plays a role in p53 stability (Kubbutat and Vousden, 1997). For this reason, we set out to examine the impact of Phe treatment on calpain expression. The results showed that Phe (100µM), unlike GI254023X and TAPI-1,

significantly decreases calpain 2 protein levels (Fig. 4A), a phenomenon that parallels a robust augmentation of p53 immunoreactivity (Fig. 4B). The examination of the effect of Phe at three different concentrations (1, 10 and 100µM), further indicated that a significant loss of calpain protein levels occurs only at 100µM (Fig. 4C) while the compound does-dependently lessens the amounts of calpain mRNA (Fig. 4D). These data indicate that Phe impairs calpain expression at a transcriptional level, thereby contributing, at least in part, to increase the levels of p53 due to a reduction in its calpain-dependent degradation with a concomitant gain of its stability.

3.5. Phe dose-dependently triggers cell cycle arrest and apoptosis

We then undertook to establish a correlation between the Phe-dependent effects upon cell cycle re-entry/arrest that is both intimately linked to neurodegeneration in brain disorders such as AD (Bonda et al., 2010) and under the tight control of p53 (Chen, 2016). We thus measured the effect of 24 hours treatment with various concentrations of Phe (1 to 100µM), using cisplatin (10µM) as a positive control of cell cycle arrest-dependent apoptosis, on the cell cycle distribution in cultured SH-SY5Y cells. The profile of p53 protein expression under these conditions displayed a Phe-induced and dose-dependent increase in p53 immunoreactivity up to 10µM followed by a decrease at 100µM that most likely reflects the fact that the peak expression of p53 has passed under conditions where massive apoptosis is most likely already underway (Fig. 5A). Analysis of the cell morphology showed a progressive loss of cell density as Phe concentrations were increased, a comparable effect being observed for 100µM of Phe and cisplatin (Fig. 5B). Furthermore, analysis of the effect of Phe on the cell cycle distribution by flow cytometry showed that concentrations ranging from 1 to 100µM gradually increased the percentage of cells in the sub-G1 phase and concomitantly decreased the number of cells in the G0/G1 phase. The distribution profiles

observed for the S and G2/M phases indicate cell cycle arrest at low Phe concentrations (1-2.5µM) and apoptosis at higher Phe concentrations (5-100µM) (Fig. 5C-D).

4. Discussion

Considering the multifactorial and complex nature of AD, multidimensional therapeutic strategies are currently adopted to prevent or slow disease progression rather than cure the disease, which often seems to be impractical (Long and Holtzman, 2019). Before any manifestation of the typical features that characterize AD pathogenesis including neuroinflammation, altered calcium homeostasis, mitochondrial dysfunction, oxidative stress and apoptosis, it is nowadays largely accepted that the seminal molecular event is an unbalanced processing of the amyloid precursor protein initiating a mechanism bringing into play synergistically toxic amyloid peptides and the hyperphosphorylated forms of Tau (Ittner and Ittner, 2018).

In this context, the redox-sensitive and metal chelator o-phenanthroline (Phe) can functionally interact with several pathways implicated in AD development. Firstly, its propensity to chelate zinc gives it the ability to inhibit the metalloproteases ADAM10 and ADAM17, which are responsible for the non-amyloidogenic processing of βAPP (Vincent and Checler, 2012). Secondly, it has been established that the tumor suppressor and pro-apoptotic protein p53 is under the positive control of Phe (Sun et al., 1997). Finally, Phe was previously reported to inhibit transcription by interfering with metal-containing DNA binding domain of specific proteins [Dizdaroglu et al., 1990; Mazumder et al., 1993). It therefore appeared relevant to us to study the impact of Phe treatment on βAPP and p53 biology and, beyond that, on cell cycle arrest in cultured human neuroblastoma cells. Importantly, the

present study was conducted using naive SH-SY5Y, thereby avoiding any possible artefacts due to protein overexpression.

Here we first showed that, although ineffective in modulating ADAM10, ADAM17 and BACE1 protein levels, GI254023X (ADAM10 specific inhibitor), TAPI-1 (ADAM17 specific inhibitor) and Phe impair sAPPα production to very different degrees. Although, GI254023X and TAPI-1 inhibition profiles were in agreement with the well-established major involvement of ADAM10 in the constitutive non-amyloidogenic processing of βAPP (Kuhn et al., 2010) compared to the subsidiary role of ADAM17, which is rather involved in the PKC-regulated α-processing of βAPP (Kim et al., 2008), the relatively weak inhibitory power of sAPPα secretion by Phe (~50%) was more surprising given that the chelation of the zinc atoms is expected to almost completely abrogate α-secretase activity. This intriguing observation finds its explanation in the fact that Phe, but neither GI254023X nor TAPI-1, significantly and dose-dependently reduced βAPP expression both at mRNA and protein levels.

The tumor suppressor p53 then appeared to be a probable intermediary between Phe and βAPP for two reasons. Firstly, it has been reported that transient expression of ectopic p53, as well as the activation of endogenous p53 by the DNA-damaging drug camptothecin or mdm2 depletion, decreases βAPP levels in several neuronal cell lines including SH-SY5Y cells by repressing βAPP promoter activity in an Sp1-dependent manner (Cuesta et al., 2009). Secondly and most interestingly, a strong (~6 fold) Phe-induced p53 transcriptional activity has been shown in a mouse epidermal tumor cell line (Sun et al., 1997). Indeed, we showed that Phe induced a significant augmentation (~3 fold) of p53 immunoreactivity with a profile that is reminiscent of that observed for βAPP down regulation. However, when measuring the impact of Phe on p53 transcription, we unexpectedly observed a significant decrease (~50%) in p53 mRNA levels at the concentrations increasing p53 protein levels. This most likely

reflects the complex regulation of the biology of p53 by Phe, which nevertheless ultimately leads, under our experimental conditions, to a strong increase in p53 protein levels and reveals a preponderant Phe-dependent post-transcriptional/post-translational positive control of p53. The additional observation by Sun and colleagues that Phe triggers p53 transcriptional activity without changing p53 mRNA or protein levels in tumor cell lines (Sun et al., 1997) further indicates that the impact of Phe on p53, beyond its complexity, could also depend on cell type.

To establish the mechanisms that could account for such an increase in protein levels, we focused on calpain, a calcium-dependent protease that possesses p53-degrading activity (Gonen et al., 1997; Pariat et al., 1997) with a particular emphasis on the ubiquitous calpain-2 (m-calpain) due to its major involvement in apoptosis (Cheng et al., 2018). The facts that Phe decreases calpain-2 protein levels at a concentration of 100µM, and dose-dependently represses calpain-2 transcription both strongly support the contention that Phe increases p53 protein levels, at least partly, via an inhibition of calpain-2-dependent p53 degradation. Although one cannot rule out a possible impact of the metal-chelating activity of Phe on calpain, this contribution could only be minor, given the low affinity of Phe for calcium. In addition, p53 stability/availability is also under the tight control of the E3 ubiquitin-protein ligase Mdm2 with the Mdm2/p53 complex being ubiquitinated before proteasome-mediated degradation of p53 (Maki et al., 1996; Kubbutat et al., 1997). An effect of Phe on this p53 regulatory pathway, although it remains to be established, cannot be excluded, as shown by the capacity of a Phe-containing organometallic compound to disrupt the Mdm2/p53 complex (Liu et al., 2016).

The demonstration that calpain inhibition leads to p53-dependent cell cycle arrest at G0/G1 and apoptosis in human tumor cells (Atencio et al., 2000) and to cell cycle arrest at G1/S (where high levels of p53 are detected) in PDGF-stimulated human fibroblasts (Dietrich

et al., 1996) led us to investigate the impact of Phe treatments on cell cycle re-entry/arrest in SH-SY5Y cells. The fact that Phe lowers cell density in a dose-dependent manner, increases p53 protein levels and promotes cell cycle arrest with similar profiles supports the triggering of cell cycle arrest by Phe, which is dependent on p53, leading to cell death by apoptosis. It is also important to stress that the lack of an effect of both GI254023X and TAPI-1 in modulating βAPP, p53 and calpain indicates that Phe operates independently of the loss of function of the α-secretases ADAM10 and ADAM17, thereby ruling out an impact of a reduction of sAPPα production on this pathway where Phe very likely acts via its metal chelating and/or DNA intercalating properties, the respective contributions of which remain to be determined.

In the light of this study, we propose a model in which Phe acts in two independent although connected modes (Fig. 6). On the one hand, Phe induces a gain in stability of p53, at least partly via a reduction in the levels of calpains, thus indirectly inhibiting the expression of βAPP (and thus sAPPα levels) and creating a vicious circle leading to an additional excess of p53, the result of which triggers cell cycle arrest. On the other hand, by reducing the production of sAPPα by inhibiting α-secretase activities, Phe leads to a decrease in the neuroprotective tone mediated by this metabolite. Ultimately, these two pathways work together to promote cell death.

Determining whether Phe operates in a similar way in non-dividing neurons deserves attention since re-entry to G1 phase by quiescent neurons was found to impart a loss of cell viability, causing significant cell death (Frade and Ovejero-Benito, 2015). In this context, it is interesting to note that, beside their p53-degrading function, calpains have been shown to activate p53 during DNA damage induced by campthothecin via the activation of the NFκB pathway in mouse primary cortical neurons (Sedarous et al., 2003).

Beyond the identification of new roles of Phe, our results also indicate that one should be careful when monitoring any impact on α-secretase activity using only sAPPα production as a read out, since some concomitant effect on the levels of its substrate βAPP is likely to lead to a false reading of the results obtained as shown here with Phe, which inhibits sAPPα production by only 25%, due to a simultaneous reduction of βAPP expression, while it reduces α-secretase catalytic activity by 50% when the hydrolysis of the specific fluorimetric substrate JMV2770 is measured.

Finally, regarding the therapeutic use of Phe-containing organometallic compounds, their promising beneficial effects in the context of therapies aimed at combating cancer (Zhao and Lin, 2005) and bacterial infections (Viganor et al., 2017) must be balanced by the present demonstration that they could at the same time promote exacerbated neuronal cell death by their ability to cross the blood-brain barrier. Nevertheless, when solely considering AD, the simultaneous targeting of βAPP processing and p53 levels could serve as a therapeutic approach since it would alleviate multiple pathological processes leading to neuronal vulnerability and death.

Acknowledgements

We would like to thank Dr Narisorn Kitiyanant (Institute of Molecular Biosciences, Mahidol University, Thailand) for providing us with the SH-SY5Y cell line, Prof. Saovaros Svasti (Institute of Molecular Biosciences, Mahidol University, Thailand) for kindly providing cisplatin and Dr Jean-Francois Hernandez (Institut des Biomolecules Max Mousseron, University of Montpellier, France) for kindly providing the fluorimetric substrate JMV2770. This work was supported by Mahidol University and The Thailand Research Fund (BRG6180002). SM was supported by a Mahidol University postdoctoral research sponsorship.

Declarations of interest: none

References

Alfa Cissé M, Gandreuil C, Hernandez JF, Martinez J, Checler F, Vincent B. (2006) Design and characterization of a novel cellular prion-derived quenched fluorimetric substrate of α-secretase. *Biochem. Biophys. Res. Commun.* 347, 254-260. https://doi.org/10.1016/j.bbrc.2006.06.065

Alves da Costa C, Sunyach C, Pardossi-Piquard R, Sevalle J, Vincent B, Boyer N, Kawarai T, Girardot N, St. Georges-Hyslop P, Checler F. (2006) Presenilin-dependent γ-secretase-mediated control of p53-associated cell death in Alzheimer's disease. *J. Neurosci.* 26, 6377-6385. https://doi.org/10.1523/jneurosci.0651-06.2006

Atencio IA, Ramachandra M, Shabram P, Demers GW. (2000) Calpain inhibitor 1 activates p53-dependent apoptosis in tumor cell lines. *Cell Growth Differ.* 11, 247-253.

Long JM, Holtzman DM. (2019) Alzheimer's disease: An update on pathobiology and treatment strategies. *Cell* 179, 312-339. https://doi.org/10.1016/j.cell.2019.09.001

Benilova I, Karran E, De Strooper B. (2012) The toxic Aβ oligomer and Alzheimer's disease: an emperor in need of clothes. *Nature Neurosci.* 15, 349-357. https://doi.org/10.1038/nn.3028

Bonda DJ, Lee HP, Kudo W, Zhu X, Smith MA, Lee HG. (2010) Pathological implications of cell cycle re-entry in Alzheimer's disease. *Expert Rev. Mol. Med.* 12:e19. https://doi.org/10.1017/s146239941000150x

Checler F, Dunys J, Pardossi-Piquard R, Alves da Costa C. (2010). p53 is regulated by and regulates members of the γ-secretase complex. *Neurodegener. Dis.* 7:50-55. https://doi.org/10.1159/000283483

Chen J. (2016) The cell cycle arrest and apoptotic functions of p53 in tumor initiation and progression. *Cold Spring Harb. Perspect. Med.* 6:a026104. https://doi.org/10.1101/cshperspect.a026104

Cheng SY, Wang SC, Lei M, Wang Z, Xiong K. (2018) Regulatory role of calpain in neuronal death. *Neural Regen. Res.* 13, 556-562. https://doi.org/10.4103/1673-5374.228762

Cuesta A, Zambrano A, Royo M, Pascual A. (2009) The tumour suppressor p53 regulates the expression of amyloid precursor protein (APP). *Biochem. J.* 418, 643-650. https://doi.org/10.1042/bj20081793

Dietrich C, Bartsch T, Schanz F, Oesch F, Wieser RJ. (1996) p53-dependent cell cycle arrest induced by N-acetyl-L-leucinyl-L-leucinyl-L-norleucinal in platelet-derived growth factor-stimulated human fibroblasts. *Proc. Natl. Acad. Sci. USA* 93, 10815-10819. https://doi.org/10.1073/pnas.93.20.10815

Dizdaroglu M, Aruoma OI, Halliwell B. (1990) Modification of bases in DNA by copper ion-1,10-phenanthroline complexes. *Biochemistry* 1990, 29, 8447-8451. https://doi.org/10.1021/bi00488a035

Folch J, Junyent F, Verdaguer E, Auladell C, Pizarro JG, Beas-Zarate C, Pallas M, Camins A. (2012) Role of cell cycle re-entry in neurons: A common apoptotic mechanism of neuronal cell death. *Neurotox. Res.* 22, 195-207. https://doi.org/10.1007/s12640-011-9277-4

Frade JM, Ovejero-Benito MC. (2015) Neuronal cell cycle: the neuron itself and its circumstances. *Cell Cycle* 14, 712-720. https://doi.org/10.1080/15384101.2015.1004937

Gonen H, Shkedy D, Barnoy S, Kosower NS, Ciechanover A. (1997) On the involvement of calpains in the degradation of the tumor suppressor protein p53. *FEBS Lett.* 406, 17-22. https://doi.org/10.1016/s0014-5793(97)00225-1

Hainaut P, Milner J. (1993) A structural role for metal ions in the "wild-type" conformation of the tumor suppressor protein p53. *Cancer Res.* 53, 1739-1742.

Hooper C, Meimaridou E, Tavassoli M, Melino G, Lovestone S, Killick R. (2007) p53 is upregulated in Alzheimer's disease and induces tau phosphorylation in HEK293a cells. *Neurosci. Lett.* 418, 34-37. https://doi.org/10.1016/j.neulet.2007.03.026

Ittner A, Ittner LM. (2018) Dendritic tau in Alzheimer's disease. *Neuron* 99, 13-27. https://doi.org/10.1016/j.neuron.2018.06.003

Jacobsen KT, Adlerz L, Multhaup G, Iverfeldt K. (2010) Insulin-like growth factor-1 (IGF-1)-induced processing of amyloid-beta precursor protein (APP) and APP-like protein 2 is mediated by different metalloproteinases. *J. Biol. Chem.* 285, 10223-10231. https://doi.org/10.1074/jbc.m109.038224

Jazvinscak Jembrek M, Slade N, Hof PR, Simic G. (2018) The interactions of p53 with tau and Aβ as potential therapeutic targets for Alzheimer's disease. *Prog. Neurobiol.* 168, 104-127. https://doi.org/10.1016/j.pneurobio.2018.05.001

Kim ML, Zhang B, Mills IP, Milla ME, Brunden KR, Lee VMY. (2008) Effects of TNFα-converting enzyme inhibition on amyloid β production and APP processing *in vitro* and *in vivo*. *J. Neurosci.* 28, 12052-12061. https://doi.org/10.1523/jneurosci.2913-08.2008

Kitamura Y, Shimohama S, Kamoshima W, Matsuoka Y, Nomura Y, Taniguchi T. (1997) Changes of p53 in the brains of patients with Alzheimer's disease. *Biochem. Biophys. Res. Commun.* 232, 418-421. https://doi.org/10.1006/bbrc.1997.6301

Kubbutat MH, Jones SN, Vousden KH. (1997) Regulation of p53 stability by Mdm2. *Nature* 387, 299-303. https://doi.org/10.1038/387299a0

Kubbutat MH, Vousden KH. (1997) Proteolytic cleavage of human p53 by calpain: a potential regulator of protein stability. *Mol. Cell. Biol.* 17, 460-468. https://doi.org/10.1128/mcb.17.1.460

Kuhn PH, Wang H, Dislich B, Colombo A, Zeitschel U, Ellwart JW, Kremmer E, Robner S, Lichtenthaler SF. (2010) ADAM10 is the physiologically relevant, constitutive α-secrertase of the amyloid precursor protein in primary neurons. *EMBO J.* 29, 3020-3032. https://doi.org/10.1038/emboj.2010.167

Lanni C, Racchi M, Mazzini G, Ranzenigo A, Polotti R, Sinforiani E, Olivari L, Barcikowska M, Styczyska M, Kuznicki J, Szybinska A, Govoni S, Memo M, Uberti D. (2008) Conformationally altered p53: a novel Alzheimer's disease marker? *Mol. Psychiatry* 13, 641-647. https://doi.org/10.1038/sj.mp.4002060

Liang SX, Richardson DR. (2003) The effect of potent iron chelators on the regulation of p53: examination of the expression, localization and DNA-binding activity of p53 and the transactivation of WAF1. *Carcinogenesis* 24, 1601-1614. https://doi.org/10.1093/carcin/bgg116

Liu LJ, He B, Miles JA, Wang W, Mao Z, Che WI, Lu JJ, Chen XP, Wilson AJ, Ma DL, Leung CH. (2016) Inhibition of the p53/hDM2 protein-protein interaction by

cyclometallated iridium (III) compounds. *Oncotarget* 7, 13965-13975. https://doi.org/10.18632/oncotarget.7369

Maki CG, Huibregtse JM, Howley PM. (1996) In vivo ubiquitination of proteasome-mediated degradation of p53. *Cancer. Res.* 56, 2649-2654.

Mazumder A, Perrin DM, Watson KJ, Sigman DS. (1993) A transcription inhibitor specific for unwound DNA in RNA polymerase-promoter open complexes. *Proc. Natl. Acad. Sci USA* 90, 8140-8144. https://doi.org/10.1073/pnas.90.17.8140

Ohyagi Y, Asahara H, Chui DH, Tsuruta Y, Sakae N, Miyoshi K, Yamada T, Kikuchi H, Taniwaki T, Murai H, Ikezoe K, Furuya H, Kawarabayashi T, Shoji M, Checler F, Iwaki T, Makifuchi T, Takeda K, Kira J, Tabira T. (2005) Intracellular Aβ42 activates p53 promoter: a pathway to neurodegeneration in Alzheimer's disease. *FASEB J.* 19, 255-257. https://doi.org/10.1096/fj.04-2637fje

Pariat M, Carillo S, Molinari M, Salvat C, Debussche L, Bracco L, Milner J, Piechaczyk M. (1997) Proteolysis by calpains: a possible contribution to degradation of p53. *Mol. Cell. Biol.* 17, 2806-2815. https://doi.org/10.1128/mcb.17.5.2806

Sedarous M, Keramaris E, O'Hare M, Melloni E, Slack RS, Elce JS, Greer PA, Park DS. (2003) Calpains mediate p53 activation and neuronal death evoked by DNA damage. *J Biol. Chem.* 2003; 278, 26031-26038. https://doi.org/10.1074/jbc.m302833200

Sun Y, Bian J, Wang Y, Jacobs C. (1997) Activation of p53 transcriptional activity by 1,10-phenanthroline, a metal chelator and redox sensitive compound. *Oncogene* 14, 385-393. https://doi.org/10.1038/sj.onc.1200834

Tan M, Wang S, Song J, Jia J. (2012) Combination of p53(ser15) and p21/p21(thr145) in peripheral blood lymphocytes as potential Alzheimer's disease biomarkers. *Neurosci. Lett.* 516, 226-231. https://doi.org/10.1016/j.neulet.2012.03.093

Uberti D, Cenini G, Olivari L, Ferrari-Toninelli G, Porrello E, Cecchi C, Pensafini A, Liguri G, Govoni S, Racchi M, Memo M. (2007) Over-expression of amyloid precursor protein in HEK cells alters p53 conformational state and protects against doxorubicin. *J. Neurochem.* 103, 322-333. https://doi.org/10.1111/j.1471-4159.2007.04757.x

Viganor L, Howe O, McCarron P, McCann M, Devereux M. (2017) The antibacterial activity of metal complexes containing 1,10-phenanthroline: Potential as alternative therapeutics in the era of antibiotic resistance. *Curr. Top. Med. Chem.* 17, 1280-1302. https://doi.org/10.2174/1568026616666161003143333

Vincent B, Checler F. (2012) α-secretase in Alzheimer's disease and beyond: Mechanistic, regulation and function in the shedding of membrane proteins. *Curr. Alzheimer Res.* 9, 140-156. https://doi.org/10.2174/156720512799361646

Vousden KH, Prives C. (2009) Blinded by the light: The growing complexity of p53. *Cell* 137, 413-431. https://doi.org/10.1016/j.cell.2009.04.037

Zhao G, Lin H. (2005) Metal complexes with aromatic N-containing ligands as potential agents in cancer treatment. *Curr. Med. Chem. Anticancer Agents* 5, 137-147. https://doi.org/10.2174/1568011053174873

Zhou X, Jia J. (2010) p53-mediated G(1)/S checkpoint dysfunction in lymphocytes from Alzheimer's disease patients. *Neurosci. Lett.* 468, 320-325. https://doi.org/10.1016/j.neulet.2009.11.024

Zhu X, Raina AK, Perry G, Smith MA. (2004) Alzheimer's disease: the two-hit hypothesis. *Lancet Neurol.* 3, 219-226. https://doi.org/10.1016/s1474-4422(04)00707-0

Legends to figures

Figure 1: Effect of phenanthroline and specific α-secretase inhibitors on sAPPα production, βAPP, ADAM10, ADAM17 and BACE1 immunoreactivities as well as on α-

secretase catalytic activity. (A) sAPPα (media) and βAPP (lysates) protein levels were measured by western blot following treatment without (control, white bar) or with GI254023X (10μM, light grey bars), TAPI-1 (10μM, dark grey bars) or Phe (100μM, black bars). Bars correspond to the densitometric analyses (βAPP being normalized with β-actin), are expressed as a percent of control taken as 100, and are the means ± SE of the indicated number of independent determinations (n). (B) The α-secretase catalytic activity was measured on cultured cells in the absence (control, white circles/white bar) or in the presence of Phe (100μM, black circles/black bar). Curves represent the mean specific fluorescence and black bar is expressed as a percentage of control (n=10). (C) ADAM10 (a), ADAM17 (b) and BACE1 (c) protein levels were measured by western blot following the indicated treatments. Bars correspond to the densitometric analyses normalized with β-actin, are expressed as a percent of control and are the means ± SE of the indicated number of independent determinations (n). * $p<0.03$; ** $p<0.02$; *** $p<0.0001$; ns, non-statistically different. The upper parts of panels (A) and (C) illustrate representative gels.

Figure 2: Five hours phenanthroline treatment alters both βAPP α-processing and βAPP expression without impairing cell viability. (A) βAPP protein levels were measured by western blot in the absence (control) or in the presence of GI254023X (10μM), TAPI-1 (10μM) or various concentrations of Phe. Bars in histogram correspond to the densitometric analyses of βAPP normalized with β-actin, are expressed as a percent of control (white bar) nd are the means ± SE of 4 to 11 independent determinations. The upper part shows one representative gel. (B) βAPP mRNA (normalized with GAPDH mRNA) were measured by real-time qPCR following treatments without or with the indicated Phe concentrations. Bars are expressed as a percentage of control (white bar) and are the means ± SE of 6 independent

determinations. (C) The α-secretase catalytic activity was measured in the absence (control, white bar) or in the presence of GI254023X (10μM, grey bar) or Phe (100μM, black bar) Bars are expressed as a percentage of control and represent the mean ± SE of 12 independent experiments. (D) shows the ratio sAPPα/βAPP (normalized with β-actin) obtained under GI254023X (10μM) or Phe (100μM) treatments. Bars are expressed as a percentage of control (white bar) and represent the means ± SEM of 7 to 11 independent determinations. (E) MTT assay following incubation without (control, white bar) or with the indicated concentrations of Phe for 5 hours. Bars represent the percentage of cell viability when compared to control untreated cells and are the means ± SEM of 15 independent measurements. * $p<0.05$; ** $p<0.002$; *** $p<0.0001$; ns, non-statistically different.

Figure 3: Phenanthroline, but not ADAM10 or ADAM17 specific inhibitors, strongly increases p53 protein amounts at a post-transcriptional level. (A) p53 immunoreactivity was measured by western blot following treatment without (control, white bar) or with GI254023X (10μM, light grey bars), TAPI-1 (10μM, dark grey bars) or Phe (100μM, black bars). Bars correspond to the densitometric analyses of p53 normalized with β-actin, are expressed as a percent of control and are the means ± SE of the indicated number of independent determinations (n). (B) p53 protein levels were measured by western blot following treatments without (control, CT) or with GI254023X (10μM), Tap-I (10μM) or the indicated concentrations of Phe. Bars correspond to the densitometric analyses of p53 normalized with β-actin, are expressed as a percent of control (white bars, non-treated cells) and are the means ± SE of 3 to 9 independent determinations (except 100μM, n=35). (C) p53 mRNA (normalized with GAPDH mRNA) were measured by real-time qPCR following treatments without or with the indicated Phe concentrations. Bars are expressed as a percentage of control (white bar) and are the means ± SE of 6 independent determinations. *

p<0.03; ** p<0.003; *** p<0.0001; ns, non-statistically different. The upper parts in (A) and (B) illustrate representative gels.

Figure 4: Phenanthroline-dependent increase in p53 immunoreactivity is accompanied by a diminution of the p53-degrading calpain2 protease. (A) Calpain2 protein levels were measured by western blot following treatment without (control, white bar) or with GI254023X (10μM, light grey bars), TAPI-1 (10μM, dark grey bars) or Phe (100μM, black bars). Bars correspond to the densitometric analyses of calpain2 normalized with β-actin, are expressed as a percent of control and are the means ± SE of the indicated number of independent determinations (n). The upper part shows one representative gel. (B) Cells were treated as in (A) in the absence (control, CT) or in the presence of Phe (100μM) and processed for p53, calpain2 and β-actin western blot. (C, D) Calpain2 protein ((normalized with β-actin, C) and mRNA (normalized with GAPDH, D) levels were measured (by western blot and real-time qPCR, respectively) following treatment without (control, white bar) or with the indicated Phe concentrations. Bars are expressed as a percentage of control (white bar) and are the means ± SE of 6 independent experiments (D) or the indicated number of independent determinations (n) (C). * p<0.002; ** p<0.0001; ns, non-statistically different.

Figure 5: Phenanthroline treatment dose-dependently induces cell cycle arrest in human neuroblastoma cells. Cultured SH-SY5Y cells were treated without (control) or various concentrations of Phe or 10 μM cisplatin (as a positive control) for 24 h. (A) Cell morphology was observed using the bright field of an inverted microscope. (B) Cell cycle analysis was undertaken using flow cytometry after staining with propidium iodide. Data is presented as the cell distribution profiles. (C) The percentage of cells in each phase is presented as mean ± Standard Deviation (SD) from three independent biological replicates.

Statistical significance for each treatment was determined as compared to control (* $p < 0.05$; ** $p < 0.01$; *** $p < 0.001$).

Figure 6: Schematic representation of the multiple effects of phenanthroline on βAPP and p53 biology leading to neuronal death. (A) represents the situation in the absence of Phe where p53 homeostasis is, at least partly, ensured by calpain-mediated p53 degradation (present study) as well as a feedback loop between p53 and βAPP (Cuesta et al., 2009). (B) illustrates the multiple actions of Phe on both βAPP and p53 biology that lead to cell cycle arrest, a loss of sAPPα-dependent neuroprotection and ultimately to neuronal death. On one hand, Phe inhibits calpain transcription, thereby reducing p53 degradation and increasing p53 protein levels. As a consequence, the feedback loop between p53 and βAPP is converted to a vicious circle that triggers runaway p53 protein production leading to cell cycle arrest On the other hand, Phe, via its zinc-chelating properties, lessens the ADAM-dependent non-amyloidogenic α-secretase processing of βAPP and impairs the production of the neuroprotective sAPPα metabolite. Interestingly, the double impact of Phe on the expression of βAPP and on the non-amyloidogenic cleavage further reduces the production of sAPPα and its neuroprotective tone. Taken as a whole, Phe, by two independent although partially connected molecular pathways, leads to p53-induced cell cycle arrest and to a loss of sAPPα-dependent neuroprotection, these combined effects resulting in neuronal death.

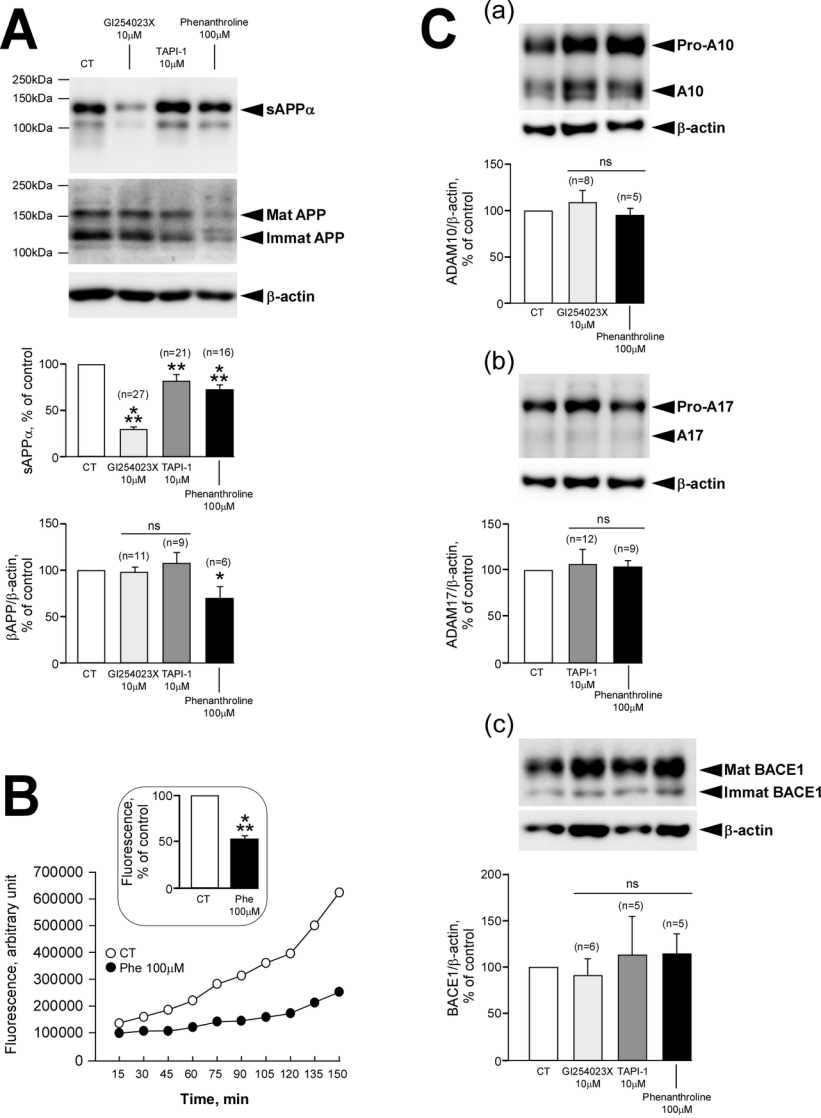
A
GI254023X 10μM
Phenanthroline 100μM
CT
TAPI-1 10μM
250kDa
150kDa
100kDa
sAPPα
Mat APP
Immat APP
β-actin
sAPPα, % of control
(n=27)
(n=21)
(n=16)
CT
GI254023X 10μM
TAPI-1 10μM
Phenanthroline 100μM
βAPP/β-actin, % of control
ns
(n=11)
(n=9)
(n=6)
B
Fluorescence, % of control
Phe 100μM
Fluorescence, arbitrary unit
CT
Phe 100μM
Time, min
C
(a)
Pro-A10
A10
β-actin
ADAM10/β-actin, % of control
(n=8)
(n=5)
(b)
Pro-A17
A17
ADAM17/β-actin, % of control
(n=12)
(n=9)
(c)
Mat BACE1
Immat BACE1
BACE1/β-actin, % of control
(n=6)
(n=5)

Figure 1

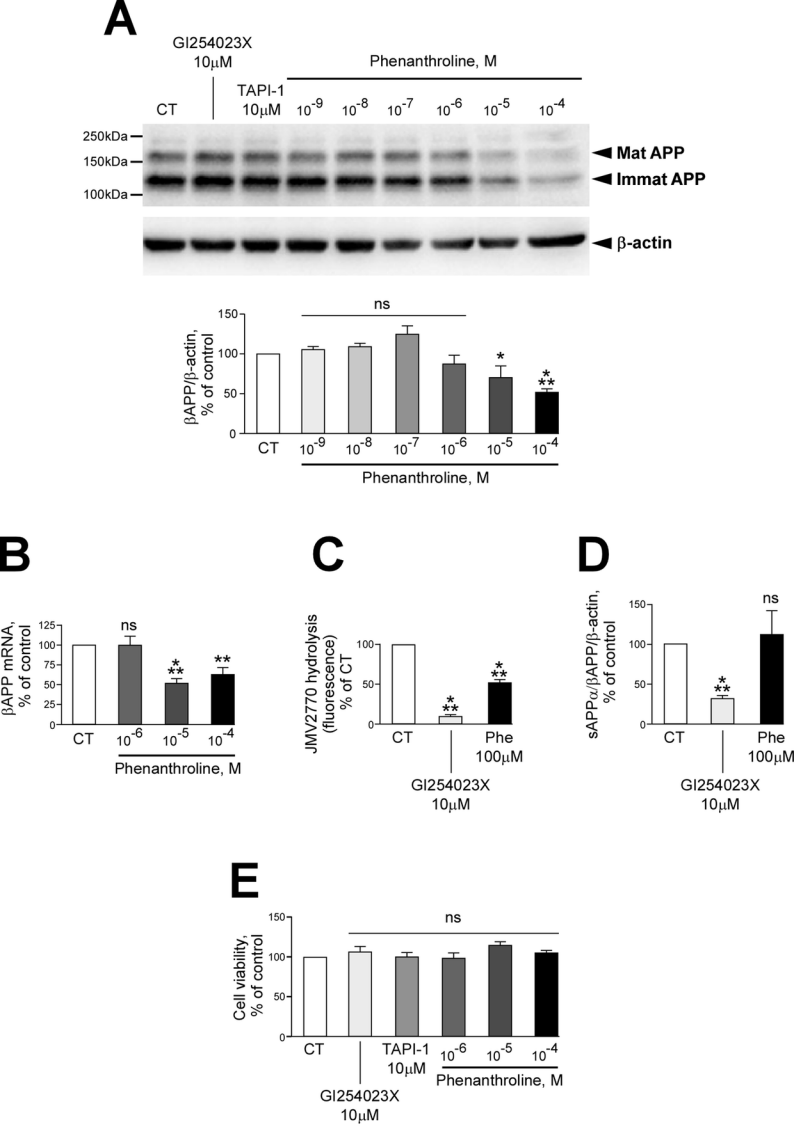
A
GI254023X
10μM
Phenanthroline, M
CT
TAPI-1
10μM
10-9
10-8
10-7
10-6
10-5
10-4
250kDa
150kDa
100kDa
Mat APP
Immat APP
β-actin
ns
βAPP/β-actin,
% of control
Phenanthroline, M
B
βAPP mRNA,
% of control
ns
Phenanthroline, M
C
JMV2770 hydrolysis
(fluorescence)
% of CT
Phe
100μM
GI254023X
10μM
D
sAPPα/βAPP/β-actin,
% of control
ns
Phe
100μM
GI254023X
10μM
E
Cell viability,
% of control
ns
TAPI-1
10μM
GI254023X
10μM
Phenanthroline, M

Figure 2

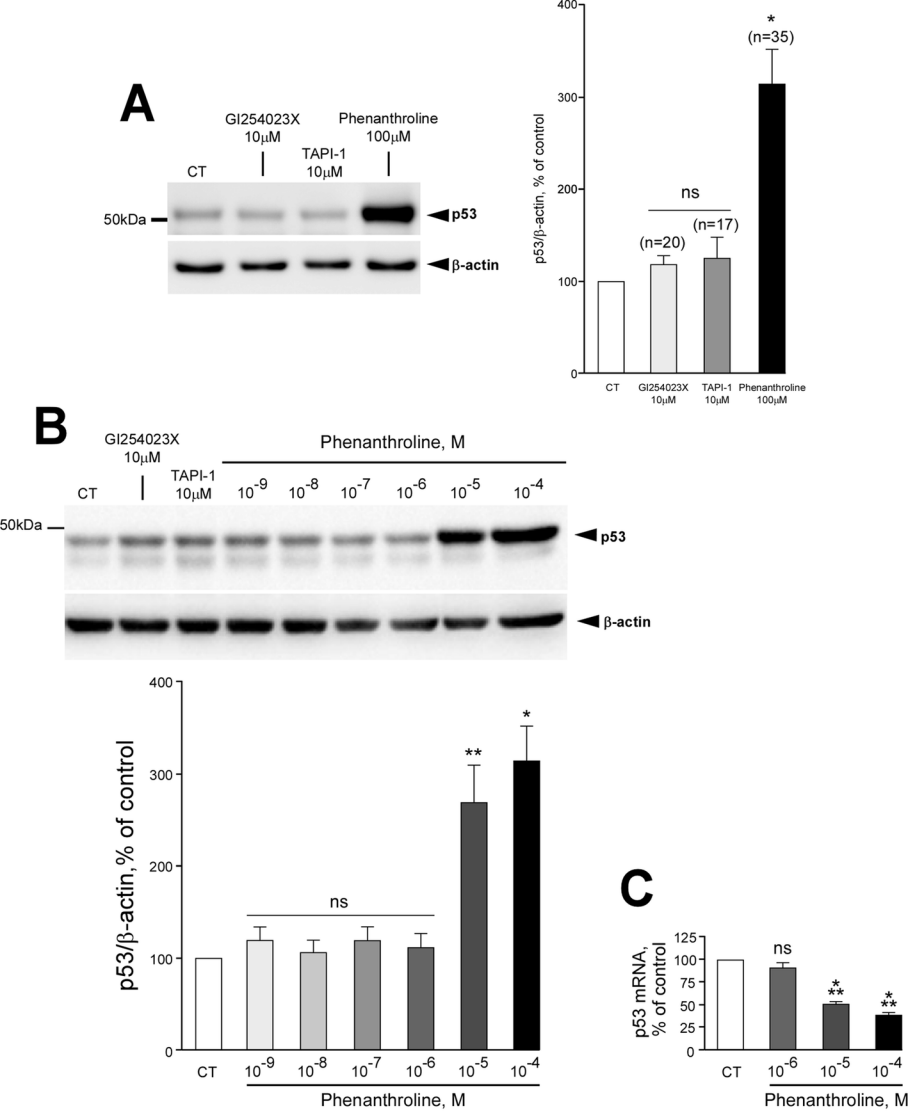
A
GI254023X
10μM
Phenanthroline
100μM
TAPI-1
10μM
CT
50kDa
p53
β-actin
p53/β-actin, % of control
ns
(n=20)
(n=17)
*
(n=35)
CT
GI254023X
10μM
TAPI-1
10μM
Phenanthroline
100μM
B
GI254023X
10μM
TAPI-1
10μM
Phenanthroline, M
CT
10-9
10-8
10-7
10-6
10-5
10-4
50kDa
p53
β-actin
p53/β-actin, % of control
ns
**
*
Phenanthroline, M
C
p53 mRNA,
% of control
ns
*
**
*
**
CT
10-6
10-5
10-4
Phenanthroline, M

Figure 3

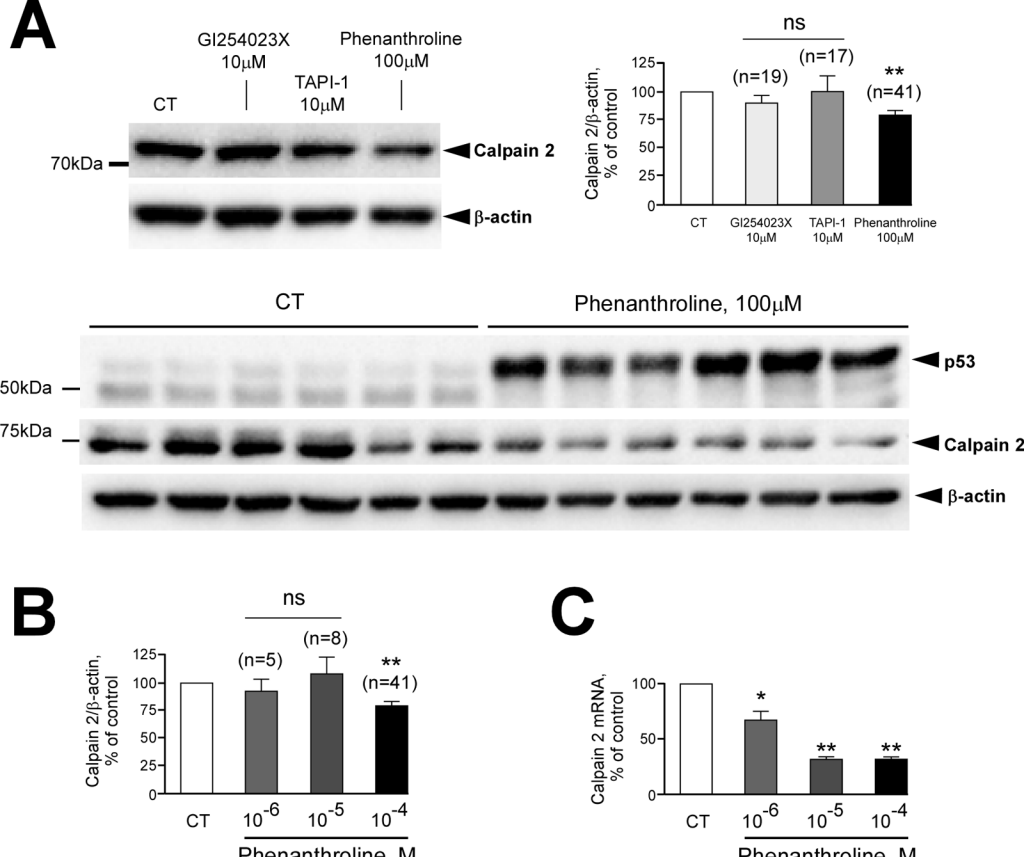
A
GI254023X
10μM
Phenanthroline
100μM
CT
TAPI-1
10μM
70kDa
Calpain 2
β-actin
ns
(n=19)
(n=17)
**
(n=41)
Calpain 2/β-actin,
% of control
125
100
75
50
25
0
CT
GI254023X
10μM
TAPI-1
10μM
Phenanthroline
100μM
CT
Phenanthroline, 100μM
50kDa
75kDa
p53
Calpain 2
β-actin
B
ns
(n=5)
(n=8)
**
(n=41)
Calpain 2/β-actin,
% of control
CT
10-6
10-5
10-4
Phenanthroline, M
C
Calpain 2 mRNA,
% of control
100
50
0
*
**
**
CT
10-6
10-5
10-4
Phenanthroline, M

Figure 4

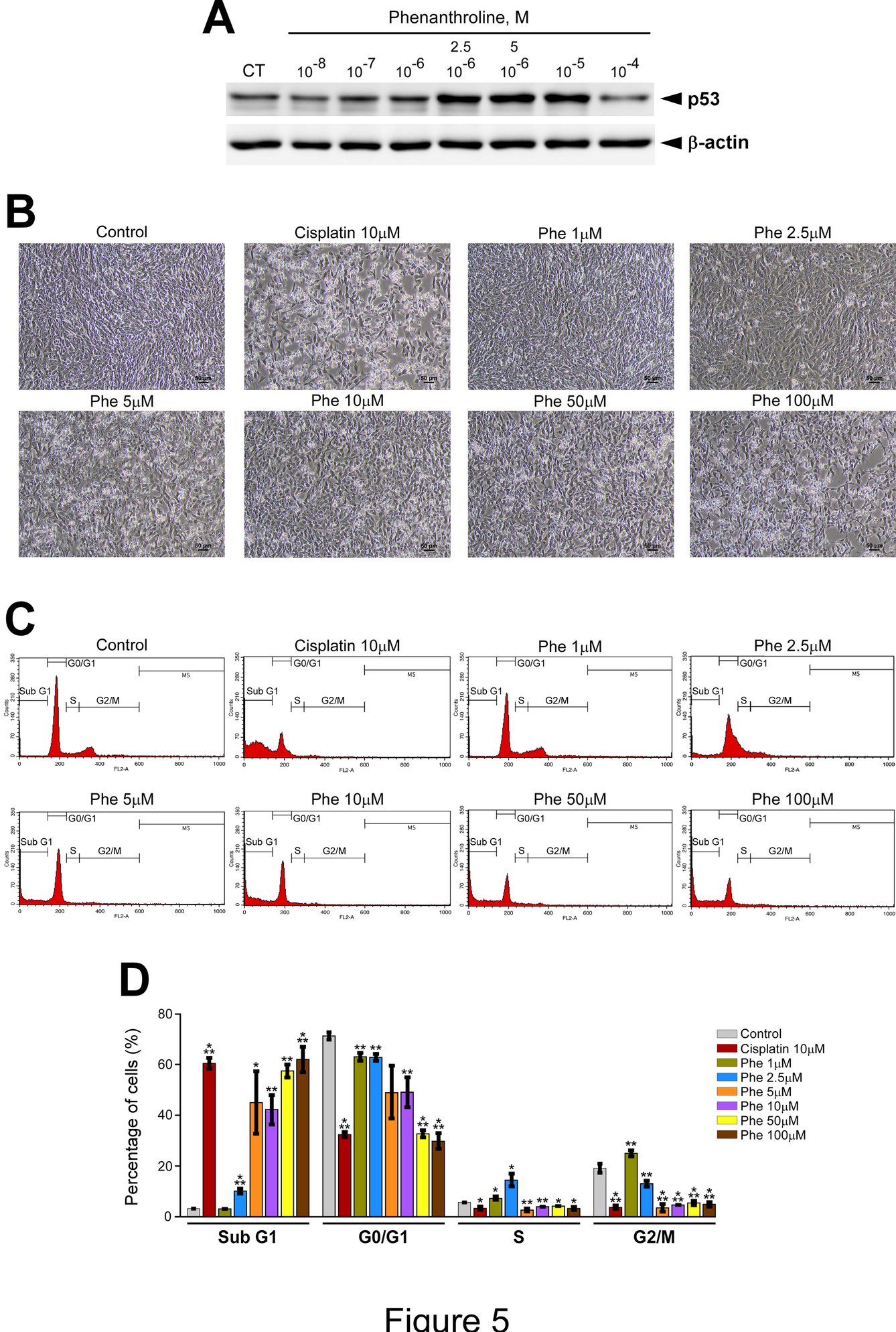
A
Phenanthroline, M
CT
10-8
10-7
10-6
2.5 10-6
5 10-6
10-5
10-4
p53
β-actin
B
Control
Cisplatin 10μM
Phe 1μM
Phe 2.5μM
Phe 5μM
Phe 10μM
Phe 50μM
Phe 100μM
50 μm
C
Control
Cisplatin 10μM
Phe 1μM
Phe 2.5μM
Phe 5μM
Phe 10μM
Phe 50μM
Phe 100μM
G0/G1
Sub G1
S
G2/M
M5
Counts
FL2-A
D
Percentage of cells (%)
Sub G1
G0/G1
S
G2/M
Control
Cisplatin 10μM
Phe 1μM
Phe 2.5μM
Phe 5μM
Phe 10μM
Phe 50μM
Phe 100μM

Figure 5

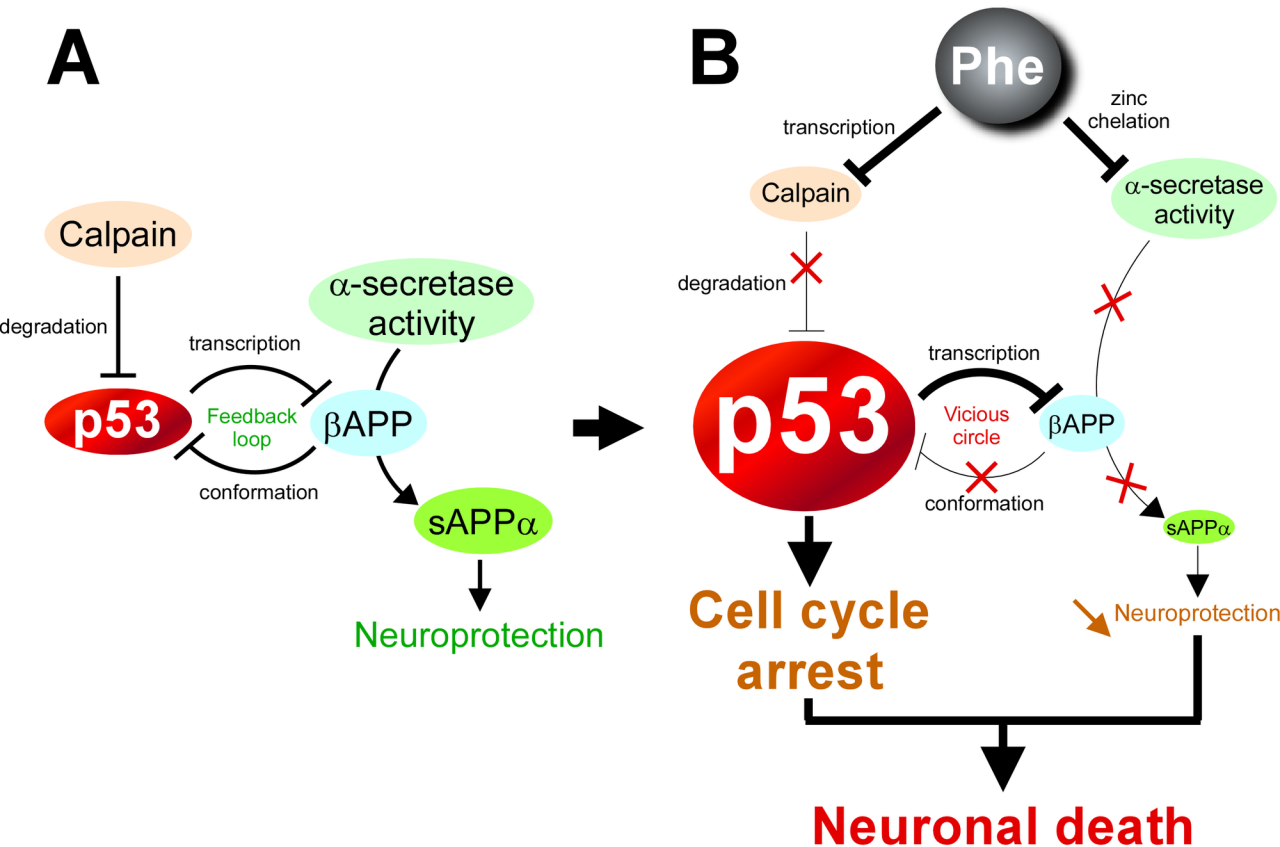
A
Calpain
degradation
p53
transcription
Feedback loop
conformation
βAPP
α-secretase activity
sAPPα
Neuroprotection
B
Phe
transcription
zinc chelation
Calpain
α-secretase activity
degradation
p53
transcription
Vicious circle
conformation
βAPP
sAPPα
Cell cycle arrest
Neuroprotection
Neuronal death

Figure 6

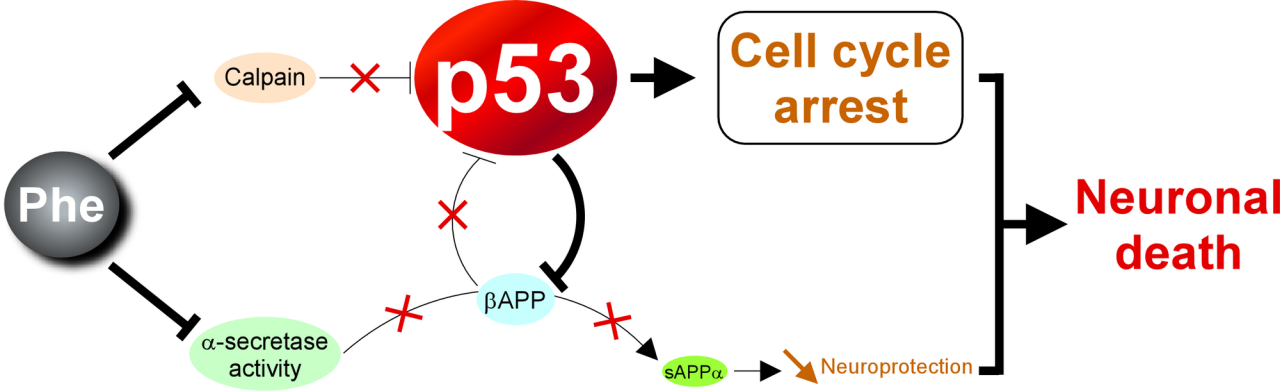
Calpain
p53
Cell cycle arrest
Phe
Neuronal death
βAPP
α-secretase activity
sAPPα
Neuroprotection